K_{ATP} channel agonists preserve connexin43 protein in infarcted rats by a protein kinase C-dependent pathway

Tsung-Ming Lee [a, *], Chih-Chan Lin [b], Hsiao-Yin Lien [c, d], Chien-Chang Chen [e, f]

[a] *Department of Medicine, Cardiology Section, Taipei Medical University and Chi-Mei Medical Center, Tainan, Taiwan*
[b] *Department of Medical Research, Chi-Mei Medical Center, Tainan, Taiwan*
[c] *Department of Pharmacy, Yongkang Veterans Hospital, Tainan, Taiwan*
[d] *Department of Cosmetic Application and Management, Tung Fang Institute of Technology, Kaohsiung, Taiwan*
[e] *Institute of Biomedical Engineering, National Cheng-Kung University, Tainan, Taiwan*
[f] *Division of Cardiovascular Surgery, Chia-yi Christian Hospital, Chia-yi City, Taiwan*

Abstract

Downward remodelling of gap junctional proteins between myocytes may trigger ventricular arrhythmia after myocardial infarction. We have demonstrated that ATP-sensitive potassium (K_{ATP}) channel agonists attenuated post-infarction arrhythmias. However, the involved mechanisms remain unclear. The purpose of this study was to determine whether K_{ATP} channel agonists can attenuate arrhythmias through preserving protein kinase C (PKC)-ϵ–dependent connexin43 level after myocardial infarction. Male Wistar rats after ligating coronary artery were randomized to either vehicle, nicorandil, pinacidil, glibenclamide or a combination of nicorandil and glibenclamide or pinacidil and glibenclamide for 4 weeks. To elucidate the role of PKCϵ in the modulation of connexin43 level, carbachol and myristoylated PKCϵ V1–2 peptide were also assessed. Myocardial connexin43 level was significantly decreased in vehicle-treated infarcted rats compared with sham. Attenuated connexin43 level was blunted after administering K_{ATP} channel agonists, assessed by immunofluorescent analysis, Western blotting, and real-time quantitative reverse transcription-PCR of connexin43. Arrhythmic scores during programmed stimulation in the K_{ATP} channel agonists-treated rats were significantly lower than those treated with vehicle. The beneficial effects of K_{ATP} channel agonists were blocked by either glibenclamide or 5-hydroxydecanoate. Addition of the PKC activator, phorbol 12-myristate 13-acetate and the specific PKCϵ agonist, carbachol, blocked the effects of nicorandil on connexin43 phosphorylation and dye permeability. The specific PKCϵ antagonist, myristoylated PKCϵ V1–2 peptide, did not have additional beneficial effects on connexin43 phosphorylation compared with rats treated with nicorandil alone. Chronic use of K_{ATP} channel agonists after infarction, resulting in enhanced connexin43 level through a PKCϵ-dependent pathway, may attenuate the arrhythmogenic response to programmed electrical stimulation.

Keywords: Arrhythmia ● connexin43 ● K_{ATP} channel agonists ● myocardial infarction ● protein kinase C

Introduction

Cardiac remodelling after myocardial infarction (MI) has been associated with gap junction heterogeneities [1], which are associated with an increased incidence of fatal arrhythmias. Connexin43 (Cx43) is the major gap junction protein with hexameric assemblies forming connexons on adjacent cardiomyocytes. Gap junction channels provide the basis for the electrical syncytial properties of the heart [2]. Gap junctions mediate the cell-to-cell movement of ions, metabolites and cell signalling molecules and may play an important role in synchronized vasoactive responses, growth responses and second-messenger signalling [3]. A reduction in gap junctional coupling between myocytes and an increase in dephosphorylation of Cx43 may be important morphological features able to induce ventricular arrhythmias in diseased myocardium [3]. Decreased ventricular Cx43 levels have been implicated in the pathogenesis of ventricular arrhythmias [4], and the engraftment of Cx43 expressing cells has been shown to prevent ventricular arrhythmias after MI [5].

*Correspondence to: Tsung-Ming LEE,
Cardiology Section, Department of Medicine,
Chi-Mei Medical Center, 901, Chung-Hwa Road,
Yang-Kan City, Tainan 710, Taiwan.
Tel.: +886-6-281-2811x52663
Fax: +886-6-283-2639
E-mail: tsungm.lee@msa.hinet.net

Recently, Rottlaender *et al.* [6] showed that Cx43 is essential for cytoprotective signal transduction on K_{ATP} channels in cardiomyocytes. Cardioprotection by both pharmacological and ischaemic pre-conditioning is abolished in transgenic animals with Cx43 deficiency [7]. Activation of K_{ATP} channels has been shown to inhibit gap junction permeability and subsequently attenuate arrhythmias in acute ischaemic myocardium [8]. However, in acute settings, the anti-arrhythmic activity with K_{ATP} channel agonists is probably a secondary effect resulting from its anti-ischaemic action [8]. In pathological situations after MI, the chronic stretch at the border zone remodels the left ventricular wall and changes the K_{ATP} channel profiles [9]. Thus, although acute administration of K_{ATP} channel agonists provides an anti-arrhythmic effect, it is unclear whether similar benefits are observed by modulating Cx43 level in chronic settings after MI.

To date, 19 phosphorylation sites have been described in Cx43 and it exists in most cells as a phosphoprotein. Cx43 phosphorylation regulates protein trafficking, assembly, and turnover as well as electrical conduction and dye permeability [10]. Serine 368 (Ser368) is phosphorylated (Cx43-pSer368) by PKC, in particular PKCε and is dephosphorylated during acute ischaemia [11]. PKCε has been identified as a component of the K_{ATP} channel signalling cascade. Jaburek *et al.* [12] showed a functional association between K_{ATP} and PKCε, and their coexistence in a multiprotein signalling complex. Previous studies have shown that activation of PKCε inhibits the function of K_{ATP} channels in vascular smooth muscle cells [13], implying that activation of K_{ATP} channels attenuates PKCε. However, whether activation of K_{ATP} channels by administering K_{ATP} channel agonists attenuates arrhythmias through preserving PKCε-dependent Cx43 phosphorylation after MI remains unknown. Thus, we assessed (1) whether K_{ATP} channel agonist administration after infarction modulates Cx43 level and attenuates ventricular arrhythmias, and (2) whether K_{ATP} channel agonists-induced Cx43 changes are PKCε dependent in a rat MI model by the use of selective inhibitors and activators of PKCε.

Materials and Methods

Animals

The animal experiment was approved and conducted in accordance with local institutional guidelines for the care and use of laboratory animals in the Chi-Mei Medical Center and conformed with the Guide for the Care and Use of Laboratory Animals published by the US National Institutes of Health (NIH Publication No. 85-23, revised 1996).

Experiment 1 (*in vivo* study).
Male Wistar rats (300–350 g) were subjected to ligation of the anterior descending artery as previously described [14], resulting in infarction of the left ventricular free wall. Twenty-four hours after induced MI, infarcted rats were randomly assigned into six groups so as to have approximately the same number of survivors in each group: (1) vehicle; (2) nicorandil

(0.1 mg/kg per day; Chugai Pharmaceutical Co., Japan), a specific mitochondrial K_{ATP} channel agonist; (3) pinacidil (0.1 mg/kg per day, Sigma-Aldrich, St. Louis, MO, USA), a non-specific K_{ATP} channel agonist; (4) glibenclamide (1.4 mg/kg per day), a K_{ATP} channel blocker; (5) a combination of nicorandil and glibenclamide and (6) a combination of pinacidil and glibenclamide. The doses of nicorandil, pinacidil and glibenclamide used in this study have been shown to specifically modulate K_{ATP} channels without interfering with haemodynamics [14]. To prevent hypoglycaemic attacks during the administration of glibenclamide, glucose was supplied and frequent glucose examinations were performed by the one-touch method. The drugs were started 24 hrs after infarction as the drugs exert maximum benefits in this time window [15]. The study duration was designed to be 4 weeks because the majority of the myocardial remodelling process in rats (70–80%) is complete within 3 weeks [16]. The drugs were given orally by gastric gavage once a day. In each-treated group, drugs were withdrawn about 24 hrs before the experiments to eliminate their pharmacological actions. Sham operation served as controls. Sham-operated rats underwent an identical procedure but without ligation of the coronary artery.

Experiment 2 (*in vitro* study)
Four weeks after induction of MI by coronary ligation, infarcted rat hearts were isolated and subjected to no treatment (vehicle), nicorandil (50 μM), pinacidil (50 μM), 5-hydroxydecanoate (5-HD, 100 μM, a mitochondrial K_{ATP} channel-selective antagonist), nicorandil + 5-HD or pinacidil + 5-HD. Each heart was perfused with a non-circulating modified Tyrode's solution containing (in mM): NaCl 117.0, NaHCO$_3$ 23.0, KCl 4.6, NaH$_2$PO$_4$ 0.8, MgCl$_2$ 1.0, CaCl$_2$ 2.0 and glucose 5.5, equilibrated at 37°C and oxygenated with a 95% O$_2$ to 5% CO$_2$ gas mixture [14]. The drugs were perfused for 30 min. The doses of nicorandil, pinacidil and 5-HD used in this study have been shown to modulate K_{ATP} channels in isolated hearts [14]. At the end of the study, all hearts ($n = 10$ each group) were used for Western blot and dye coupling at the border zone (<2 mm within the infarct).

Experiment 3 (*in vitro* study)
The *in vitro* approach was used to further study intracellular signalling pathways of Cx43 regulation and to elucidate the role of PKCε in the modulation of cardiac Cx43 level by K_{ATP} channel activation. Infarcted hearts 4 weeks after MI were isolated and subjected to no treatment (vehicle), nicorandil (50 μM), nicorandil + phorbol 12-myristate 13-acetate (PMA, 0.1 μM, a PKC agonist), nicorandil + chelerythrine (50 nM, a PKC antagonist), nicorandil + carbachol (100 μM, a PKCε-selective agonist; Sigma-Aldrich) or nicorandil + myristoylated PKCε V1–2 peptide (1 μM, εV1–2, a PKCε-selective antagonist; Biomol Research, Plymouth, PA, USA). Each heart was perfused as in Experiment 2, and the drugs were also infused for 30 min. The doses of PMA [17], chelerythrine [12], carbachol [18] and εV1–2 [19] used have been shown to effectively modulate PKC. At the end of the study, all hearts were used for Western blot for Cx43 and dye coupling at the border zone.

Haemodynamics and infarct size measurements

Haemodynamic parameters were measured in anaesthetized rats with ketamine (90 mg/kg) intraperitoneally at the end of the study. A polyethylene Millar catheter was inserted *via* the right carotid artery and connected to a transducer (Model SPR-407; Miller Instruments, Houston, TX, USA) to measure left ventricular systolic and diastolic pressure as the mean of measurements of five consecutive pressure cycles as previously described

[14]. The maximal rate of left ventricular pressure rise ($+\mathrm{d}p/\mathrm{d}t$) and decrease ($-\mathrm{d}p/\mathrm{d}t$) was measured. After the arterial pressure measurement, the heart was paced for the *in vivo* electrophysiological tests. At completion of the electrophysiological tests, the atria and the right ventricle were trimmed off, and the LV was rinsed in cold physiological saline, weighed and immediately frozen in liquid nitrogen after obtaining a coronal section of the left ventricular for infarct size estimation. A section, taken from the equator of the left ventricular, was fixed in 10% formalin and embedded in paraffin for determination of infarct size. Each section was stained with haemotoxylin and eosin, and trichrome. Infarct size (%) was expressed as the ratio of the sum of external and internal perimeters of left ventricular as described by Pfeffer and Braunwald [20]. With respect to clinical importance [20], only rats with large infarction ($>30\%$) were selected for analysis.

In vivo electrophysiological studies

After the arterial pressure measurement, the rats were intubated, and artificially ventilated with humidified room air supplemented with oxygen. Because the residual neural integrity at the infarcted site is one of the determinants of the response to electrical induction of ventricular arrhythmias [21], only rats were included with the infarcted area of the left ventricular totally replaced by scar tissue. Body temperature was maintained at 37°C by a thermostatically controlled heated lamp. Programmed electrical stimulation was performed through electrodes sewn on the epicardial surface of the right ventricular outflow tract. Induced arrhythmias were effected using an electrical Bloom stimulator. To induce ventricular arrhythmias, eight paced beats at a cycle length of 120 msec. (S_1) were applied, followed by one to three extrastimuli (S_2, S_3 and S_4) at shorter coupling intervals. The end point of ventricular pacing was induction of ventricular tachyarrhythmia. Ventricular tachyarrhythmias including ventricular tachycardia and ventricular fibrillation were considered non-sustained when it lasted ≤ 15 beats and sustained when it lasted >15 beats. An arrhythmia scoring system was modified as previously described [14]: 0, non-inducible preparations; 1, non-sustained tachyarrhythmias induced with three extrastimuli; 2, sustained tachyarrhythmias induced with three extrastimuli; 3, non-sustained tachyarrhythmias induced with two extrastimuli; 4, sustained tachyarrhythmias induced with two extrastimuli; 5, non-sustained tachyarrhythmias induced with one extrastimulus; 6, sustained tachyarrhythmias induced with one extrastimulus and 7, tachyarrhythmias induced during the eight paced beats. If the heart stopped before the pacing, the arrhythmia score assigned to that heart was 8. The experimental electrophysiological protocols were typically completed within 10 min.

Determination of gap junction permeability

Gap junction permeability at the border zone (<2 mm within the infarct) was determined by using Lucifer yellow according to the method of Ruiz-Meana *et al.* [22] with slight modification. In brief, the left ventricular at the border zone was excised in Experiments 2 and 3 and an incision was quickly made in the endocardium. The left ventricular was then immediately soaked and incubated in Krebs–Henseleit buffer containing Lucifer yellow (2.5 mg/ml) and rhodamine-conjugated dextran (2.5 mg/ml), which was continuously bubbled with a 95% O_2–5% CO_2 gas mixture, for 30 min. at 37°C. Then, the left ventricular was fixed with 1% glutaraldehyde to 4% formaldehyde in 0.2M cacodylate buffer (pH 7.4). The Lucifer yellow- and rhodamine-labelled regions were quantitatively measured from 10 randomly selected fields at a magnification of $100\times$ by computerized planimetry (Image Pro Plus; Media Cybernetics, Silver Spring, MD, USA).

The value was expressed as the ratio of the difference between Lucifer yellow-labelled area and rhodamine-labelled area to rhodamine-labelled area. The slides were coded so that the investigator was blinded to the rat identification.

Real-time RT-PCR of Cx43

Real-time quantitative reverse transcription-PCR (RT-PCR) was performed from samples obtained from the border zone with the TaqMan system (Prism 7700 Sequence Detection System; PE Biosystems, Foster City, CA, USA) as previously described [14]. For Cx43, the primers were 5′-TGAAAGAGAGGTGCCCAGACA-3′ (sense) and 5′-CGTGAG AGATGGGGAAG-GACT-3′ (antisense). For cyclophilin, the primers were 5′-ATGGTCAACCC-CACCGTGTTCTTCG-3′ and 5′-CGTGTGAAGTCACCACCCTGACACA-3′. Cyclophilin mRNA was chosen as the internal standard because it is expressed at a constant level in virtually all tissues. Standard curves were plotted with the threshold cycles *versus* log template quantities. For quantification, Cx43 level was normalized to the expressed cyclophilin. Reaction conditions were programmed on a computer linked to the detector for 40 cycles of the amplification step. The results of the real-time RT-PCR assay were expressed as the Ct value, defined as the cycle number at which the sample passed a fixed fluorescence threshold and became positive. For each cDNA sample, the Ct value of the reference gene cyclophilin was subtracted from the Ct value of the sample to obtain ΔCt. Relative expression levels were calculated using the formula $\Delta\Delta$Ct $= \Delta$Ct (treated) $- \Delta$Ct (sham), and the value used to plot the relative level was calculated using the expression $2^{-\Delta\Delta Ct}$. Experiments were replicated three times and results expressed as the mean value.

Western blot analysis of total Cx43, Cx43-pSer368 and PKCε

Samples obtained from the border zone were homogenized. The supernatant protein concentration was determined with the BCA protein assay reagent kit (Pierce Endogen, Rockford, IL, USA). Twenty micrograms of protein was separated by 10% SDS-PAGE and electrotransferred onto a nitrocellulose membrane. The nitrocellulose membrane was then rinsed with a blocking solution of 5% non-fat dry milk and incubated with anti-total Cx43 (1:250, #71-0700; Zymed, San Francisco, CA, USA), anti-Cx43-pSer368 (1:250; Chemicon, Temecula, CA, USA), anti-phospho-PKCε^{Ser729} (pPKCε, sc-12355; 1:500, Santa Cruz, CA, USA) and anti-PKCε (sc-214, Santa Cruz; 1:500) antibodies. Antigen–antibody complexes were detected with 5-bromo-4-chloro-3-indolyl-phosphate and nitroblue tetrazolium chloride (Sigma-Aldrich). Films were volume-integrated within the linear range of the exposure using a scanning densitometer. Relative abundance was obtained by normalizing the density of Cx43 protein against that of β-actin. Experiments were replicated three times and results expressed as the mean value.

Immunofluorescent studies of Cx43

To investigate the spatial distribution and quantification of Cx43, analysis of immunofluorescent staining was performed on left ventricular muscle from the border zone and the remote zone (≥ 2 mm outside the infarct). Paraffin-embedded sections were performed at a thickness of 5 μm. Tissues were incubated with Cx43 antibodies (1:200, #71–0700; Zymed) in 0.5% BSA in PBS overnight at 37°C. The second antibody was monoclonal goat anti-mouse IgG conjugated to fluorescein isothiocyanate (FITC, Sigma-Aldrich), at 1:50 dilution in PBS containing 0.5% BSA for 1 hr. The sections were washed three times with PBS and mounted in Dako fluorescent mounting medium. Isotype-identical directly conjugated antibodies served as a negative control.

Table 1 Cardiac morphology, haemodynamics, glucose and insulin levels at the end of study

Parameters	Sham	Infarction treated with					
		Vehicle	Nic	Pin	Glib	Nic + Glib	Pin + Glib
No. of rats	12	10	11	12	10	10	12
Body weight, (g)	412 ± 15	420 ± 12	415 ± 15	410 ± 11	417 ± 12	418 ± 12	416 ± 11
Heart rate (bpm)	406 ± 12	416 ± 15	414 ± 14	408 ± 12	419 ± 14	404 ± 13	410 ± 17
LVESP (mm Hg)	106 ±5	105 ± 9	101 ± 8	102 ± 12	114 ± 7	103 ± 9	104 ± 10
LVEDP (mm Hg)	6 ± 1	18 ± 2	15 ± 4	16 ± 5	20 ± 5	19 ± 7	19 ± 5
+dp/dt (mm Hg/sec.)	6672 ± 254[#]	2755 ± 312	3593 ± 275*	3629 ± 268*	2687 ± 273	2498 ±265	2693 ± 238
−dp/dt (mm Hg/sec.)	6456 ± 275[#]	1833 ± 230*	3170 ±238*	2988 ± 236*	2017 ±212	2271 ± 282	2182 ± 192
Infarct size (%)	0	40 ± 4	41 ± 3	38 ± 3	40 ± 3	40 ± 4	41 ± 2
LVW/BW (mg/g)	2.07 ± 0.21[‡]	2.99 ± 0.22	2.89 ± 0.33	2.95 ± 0.32	3.05 ± 0.33	3.11 ± 0.23	3.03 ± 0.29
RVW/BW (mg/g)	0.51 ± 0.05*	0.79 ± 0.10	0.53 ± 0.07*	0.55 ± 0.09*	0.73 ± 0.10	0.72 ± 0.14	0.73 ± 0.12
LungW/BW (mg/g)	4.16 ± 0.34*	5.54 ± 0.48	4.41 ± 0.50*	4.49 ± 0.41*	5.24 ± 0.39	5.29 ± 0.54	5.64 ± 0.37
Glucose (mg/dl)	85 ± 4	87 ± 5	84 ± 6	86 ± 7	83 ± 8	86 ± 9	85 ± 9
Insulin (μu/ml)	26 ± 5[‡]	53 ± 9	52 ± 12	49 ± 16	155 ± 22[†††]	137 ± 25[†††]	137 ± 19[†††]

Values are mean ± S.D.

BW: body weight; Glib: glibenclamide; LungW: lung weight; LVEDP: left ventricular end-diastolic pressure; LVESP: left ventricular end-systolic pressure; LVW: left ventricular weight; Nic: nicorandil; Pin: pinacidil; RVW: right ventricular weight. *$P < 0.05$ compared with vehicle, glibenclamide, nicorandil + glibenclamide and pinacidil + glibenclamide; [†††]$P < 0.001$ compared with vehicle, nicorandil and pinacidil; [‡]$P < 0.05$, [#]$P < 0.01$ compared with all infarcted groups.

The density of Cx43-labelled regions was qualitatively estimated from 10 randomly selected fields at a magnification of 400×. The density was measured on the tracings by computerized planimetry (Image Pro Plus, Media Cybernetics). To eliminate artifactual quantification of Cx43 protein, samples were discarded when the imaging plane was not parallel to the long axis of the fibre. The value was expressed as the ratio of Cx43-labelled area to total area. The slides were coded so that the investigator was blinded to the rat identification.

Laboratory measurements

To determine the confounding roles of glucose and insulin in Cx43 remodelling, blood samples from the aorta were assayed at the end of the study. Plasma insulin concentration was measured by collecting 4 ml of blood in test tubes containing 2% ethylenediaminetetraacetic acid (80 μl/ml of blood). Blood samples were immediately centrifuged at 3000 × g for 10 min., and the plasmas were stored at –70°C until further analysis. Insulin was measured by ultrasensitive rat enzyme immunoassay (Mercodia, Uppsala, Sweden).

Statistical analysis

Results were presented as mean ± S.D. Statistical analysis was performed with the SPSS statistical package (version 12.0; SPSS, Chicago, IL, USA). Differences among the groups of rats were tested by a one-way ANOVA. Subsequently, analysis for significant differences between the two groups was performed with a multiple comparison test (Scheffe's method).

Electrophysiological data (scoring of programmed electrical stimulation-induced arrhythmias) were compared by a Kruskal–Wallis test followed by a Mann–Whitney test. Interaction term of nicorandil, pinacidil and glibenclamide effects was incorporated into the model. Relationships between the changes were studied by use of Spearman correlation. The significant level was assumed at value of $P < 0.05$.

Results

Differences in mortality among the infarcted groups (vehicle, $n = 15$, 60%; nicorandil, $n = 13$, 54%; pinacidil, $n = 14$, 54%; glibenclamide, $n = 18$, 64%; nicorandil ± glibenclamide, $n = 14$, 58%; pinacidil ± glibenclamide, $n = 13$, 52%) were not found throughout the study. Either nicorandil, pinacidil, or glibenclamide had little effect on cardiac gross morphology in the sham-operated rats (data not shown). Four weeks after infarction, the infarcted area of the LV was very thin and was totally replaced by fully differentiated scar tissue. The weight of the left ventricular inclusive of the septum remained essentially constant 4 weeks among the infarcted groups (Table 1). Compared with vehicle-treated infarcted rats in nicorandil- or pinacidil-treated infarcted rats, right ventricular weight/body weight ratio and lung weight/body weight ratio were significantly lower, consistent with favourable left ventricular remodelling. LV end-systolic pressure and infarct size did not
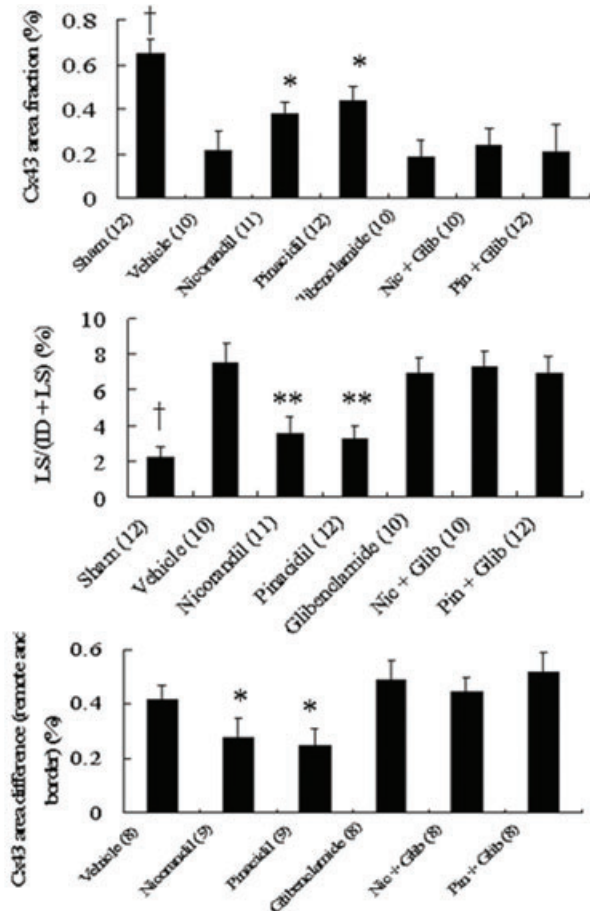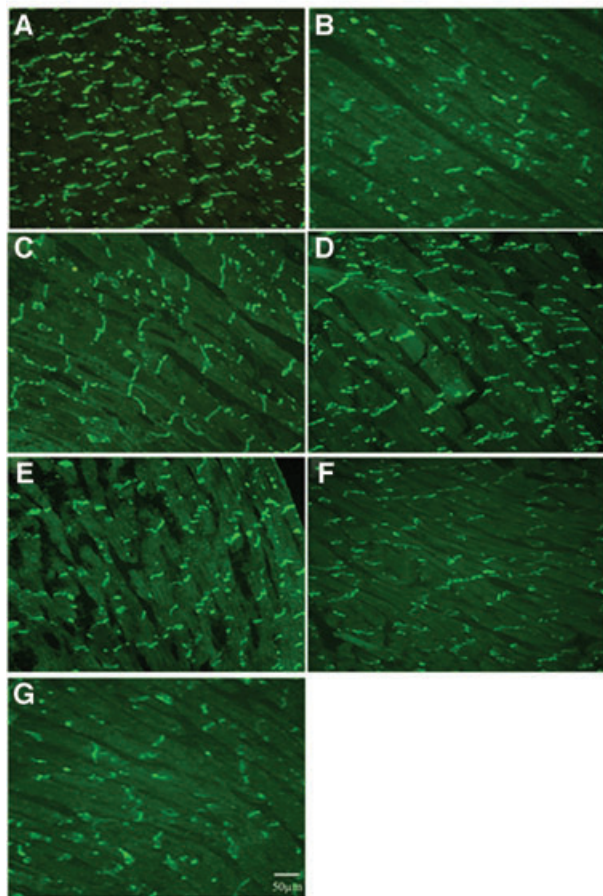
Fig. 1 Immunofluorescent staining for Cx43 from the border zone (magnification 400×). Infarction markedly decreased Cx43 level. After administering either nicorandil or pinacidil, Cx43 signals were increased. (**A**) Sham; (**B**) vehicle; (**C**) nicorandil (Nic); (**D**) pinacidil (Pin); (**E**) glibenclamide (Glib); (**F**) Nic + Glib; (**G**) Pin + Glib. Bar = 50 μm. The number of animals in each group is indicated in parentheses. ID: intercalated disk; LS: lateral cell surface. *$P < 0.05$, **$P < 0.01$ compared with vehicle-, Glib-, Nic + Glib- and Pin + Glib-treated groups. †$P < 0.05$ compared with infarcted groups.

differ among the infarcted groups. Insulin concentrations were significantly increased in rats administered with glibenclamide.

Immunofluorescent studies of Cx43

In the sham group, sections stained with the Cx43 antibody produced intense punctate labelling primarily at intercalated discs between cardiomyocytes (Fig. 1). Infarction resulted in a significant decrease in total amount of Cx43 immunoreactive signals of 66%. The ratio of Cx43 area to the total area was significantly increased in nicorandil- and pinacidil-treated rats compared to vehicle-treated rats (73% for nicorandil and 92% for pinacidil; Fig. 1). The ratio of Cx43 immunofluorescence at the lateral cell surface to the entire cell surface was significantly lower in nicorandil- and pinacidil-treated rats than in vehicle-treated rats ($3.65 \pm 0.86\%$ for nicorandil, $3.29 \pm 0.69\%$ for pinacidil *versus* $7.56 \pm 1.06\%$, $P < 0.01$). The changed level of K$_{ATP}$ chan-

nel agonist-related Cx43 could be reversed to the level, similar to the vehicle-treated rats after adding glibenclamide. In addition, there were no significant differences in Cx43 levels at the remote zone among the infarcted groups. Differences in Cx43 levels between the border zone and remote area were significantly lower in the infarcted groups treated with K$_{ATP}$ channel agonists (Fig. 1).

Western blot and real-time RT-PCR

Two predominant forms of Cx43 were detected (Fig. 2); a non-phosphorylated form (P0) and a phosphorylated species (P1). The P1/P0 ratio was used as the magnitude of the phosphorylation of Cx43. Western blot analysis derived from the border zone revealed that the P1/P0 ratio was significantly decreased in response to infarction. Ventricular remodelling was associated with a markedly decreased amount of phosphorylated- and total Cx43 at the border zone. In the K$_{ATP}$ channel agonist-treated
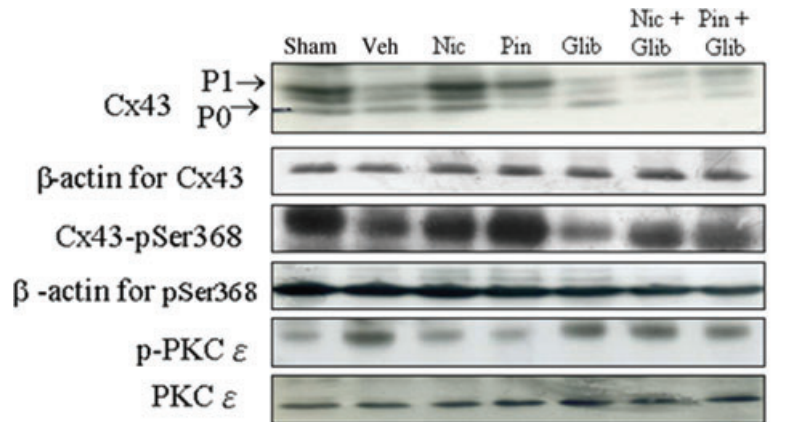
Fig. 2 Experiment 1. *In vivo* effect of K_{ATP} channel agonists on Western blot using antibodies: total Cx43, antibody against the carboxy terminal part of Cx43; Cx43-pSer368, phospho-specific antibody to detect Cx43 phosphorylation on Ser368; p-PKCε and PKCε, antibody detecting phosphor- and total PKCε, respectively. Ventricular remodeling after MI was associated with a markedly decreased amount of phosphorylated Cx43 (P1). Significantly increased Cx43 amount, P1/P0 ratio and Cx43-pSer368 took place in the groups treated with nicorandil (Nic) or pinacidil (Pin) compared with the vehicle. Each point is an average of three separate experiments. Relative abundance was obtained by normalizing the density of Cx43 protein against that of β-actin. The number of animals in each group is indicated in parentheses. P0: non-phosphorylated Cx43; P1: phosphorylated Cx43. *$P < 0.05$, **$P < 0.01$ compared with infarcted groups; †$P < 0.05$ compared with the vehicle-, Glib-, Nic + Glib- and Pin + Glib-treated groups; ‡‡$P < 0.001$ compared with sham.
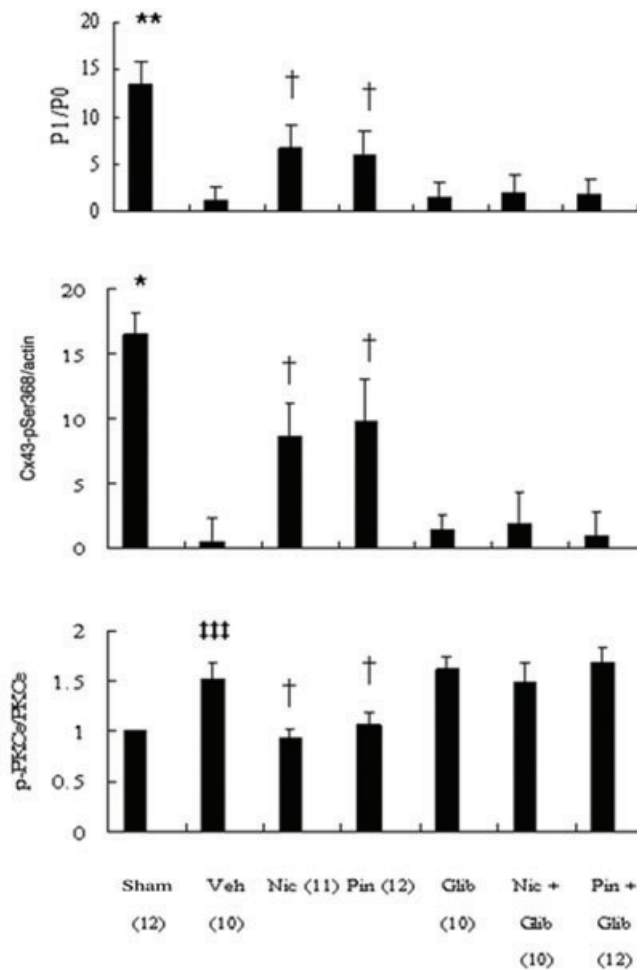
groups, the level of total Cx43 was maintained at 50% for nicorandil and 44% for pinacidil of that in the sham group. The enhanced level of K_{ATP} channel agonist-related Cx43 could be reversed to the levels similar to the vehicle-treated infarcted rats after adding glibenclamide. Although K_{ATP} channel antagonist-induced Cx43 expression was altered at four weeks after infarction, glibenclamide was used as an antagonist of K_{ATP} channels as it can block both mitochondrial and sarcolemmal K_{ATP} channels
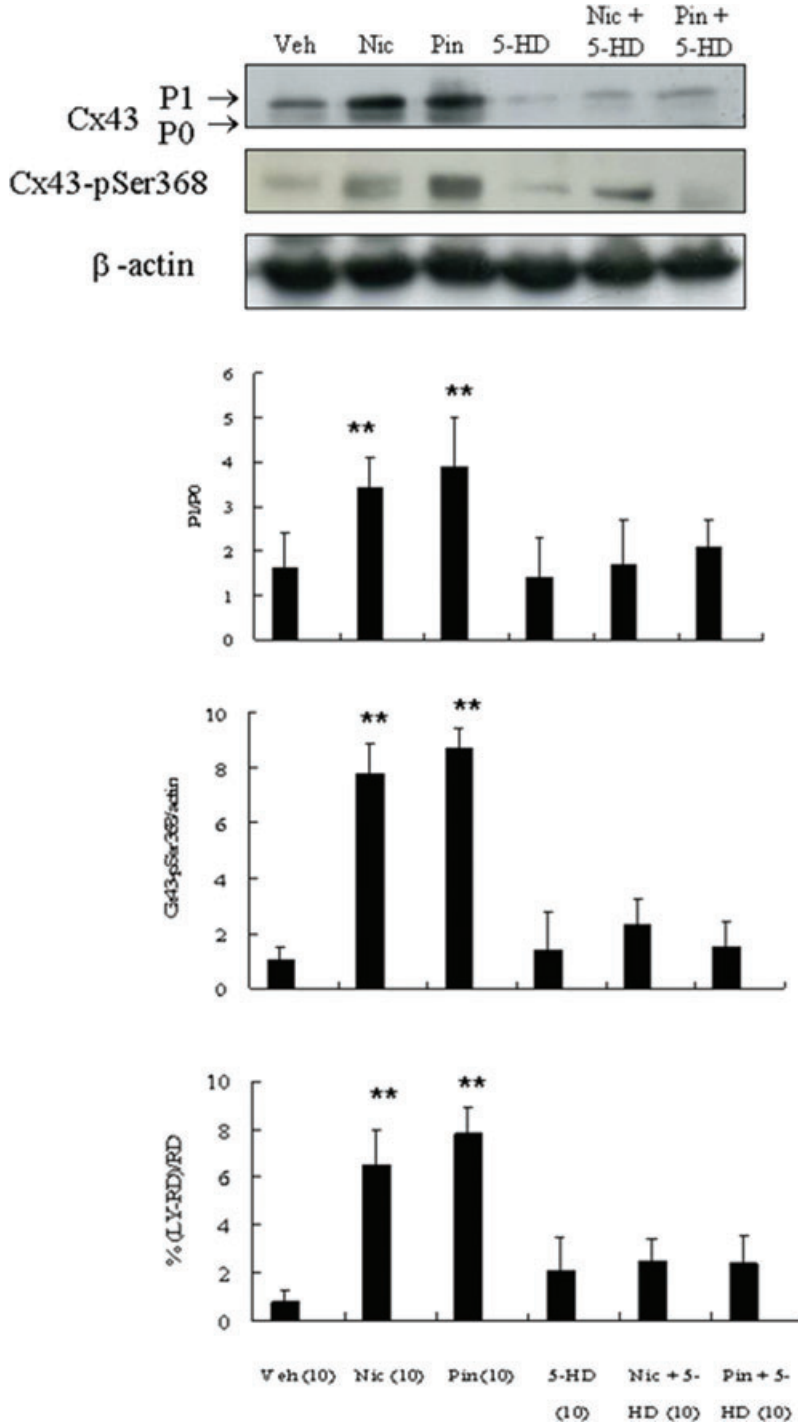
Fig. 3 Experiment 2. In a rat isolated heart model, the effect of mitochondrial K_{ATP} channel agonists on gap junctional communication and Western blot using antibodies: total Cx43 and Cx43-pSer368. Significantly decreased Cx43 amount, P1/P0 ratio and gap junctional communication were noted in the group treated with 5-HD compared with nicorandil (Nic) or pinacidil (Pin) alone. Relative abundance was obtained by normalizing the density of Cx43 protein against that of β-actin. Each point is an average of three separate experiments ($n = 10$ per group). LY: Lucifer yellow; P0: non-phosphorylated Cx43; P1: phosphorylated Cx43; RD: rhodamine-conjugated dextran. $**P < 0.01$ compared with vehicle- and 5-HD–treated groups.

and has multiple actions independent of K_{ATP} channels. To elucidate the role of mitochondrial K_{ATP} channels in modulating Cx43, 5-HD was assessed in an *in vitro* model. Figure 3 shows that 5-HD significantly the decreased level of Cx43 compared with either nicorandil or pinacidil alone, confirming the role of mitochondrial K_{ATP} channels in mediating Cx43 level. Furthermore, either PMA or carbachol suppressed the nicorandil-induced enhanced Cx43 level (Fig. 4).
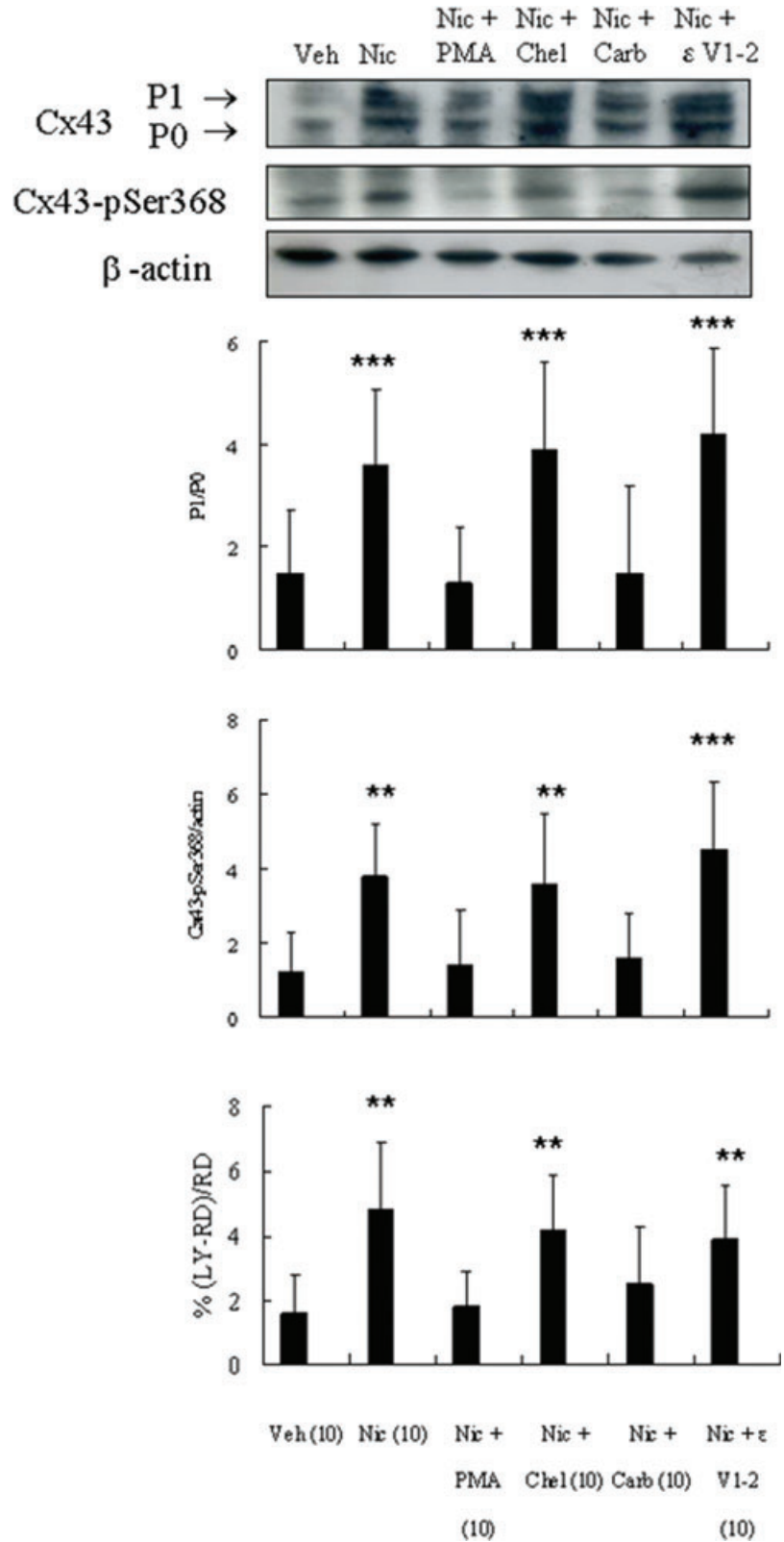
Fig. 4 Experiment 3. In a rat isolated heart model, the effect of PKCε on K_{ATP} channel agonist-induced gap junctional communication and Western blot using antibodies: total Cx43 and Cx43-pSer368. Significantly reduced Cx43 amount, P1/P0 ratio and gap junctional communication were noted in the groups treated with nicorandil (Nic) + PMA or Nic + carbachol compared with Nic alone. Relative abundance was obtained by normalizing the density of Cx43 protein against that of β-actin. Each point is an average of three separate experiments ($n =$ 10 per group). Carb: carbachol; Chel: chelerythrine; LY: Lucifer yellow; P0: non-phosphorylated Cx43; P1: phosphorylated Cx43; PMA: phorbol 12-myristate 13-acetate; RD: rhodamine-conjugated dextran; εV1–2: myristoylated PKCε V1–2 peptide myristoylated PKCε V1–2 peptide. $**P < 0.01$, $***P < 0.001$ compared with groups treated with vehicle, Nic + PMA and Nic + Carb.
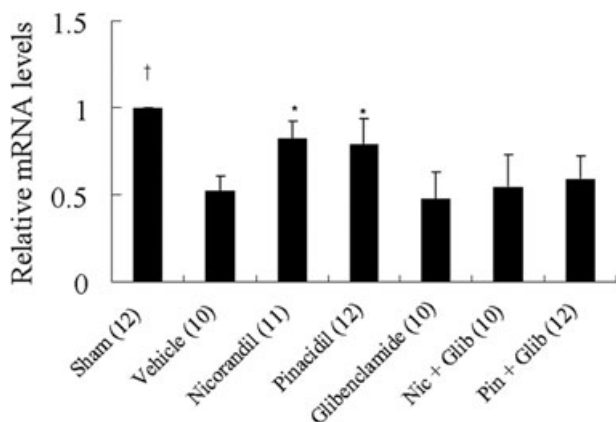
Thereafter, we examined the effect of K_{ATP} channel agonists on Cx43-pSer368. Analysis of immunoblots revealed a significant decrease in the amount of Cx43-pSer368 at the border zone in the vehicle-treated infarcted rats compared with the sham-operated rats (Fig. 2). To further elucidate the role of K_{ATP} channel agonist-related PKCε in modulating Cx43 level, carbachol was assessed in an *in vitro* model. Figure 4 shows that carbachol significantly decreased the level of Cx43-pSer368 compared with nicorandil-treated rats alone, confirming the role of PKCε in mediating Cx43-pSer368 level.

Western blot showed that the levels of left ventricular phospho-PKCε were significantly up-regulated 1.52-fold at the border zone in the vehicle compared to the sham-operated rats ($P < 0.001$),

whereas total PKCε remained constant (Fig. 2). Compared with the vehicle in nicorandil- and pinacidil-treated rats, left ventricular phospho-PKCε levels were significantly lower at the border zone. The rats to which glibenclamide were administered showed significantly higher phospho-PKCε levels than those in the nicorandil- and pinacidil-treated groups alone. The linear regression models showed that the fold increase of phospho-PKCε/total PKCε significantly correlated with the levels of P1/P0 ($r = -0.53$, $P = 0.01$) and Cx43-pSer368 ($r = -0.48$, $P = 0.02$).

The Cx43 mRNA levels showed a significant down-regulation at the border zone in the vehicle compared with the sham-operated rats (Fig. 5). In either nicorandil- or pinacidil-treated infarcted rats, the Cx43 mRNA levels were significantly increased compared with those in the vehicle. The increased magnitude of Cx43 mRNA levels was blunted in combination therapy of nicorandil + glibenclamide compared to that in nicorandil-treated alone.

Effects of K_{ATP} channel agonists on the gap junction permeability

As shown in Figures 3 and 6, vehicle-treated infarcted rats showed a significantly reduced gap junction permeability compared with rats treated with either nicorandil or pinacidil. This beneficial effect of K_{ATP} channel agonists was abolished by 5-HD, suggesting that the effect of K_{ATP} channel agonists on gap junction permeability was mediated by opening of mitochondrial K_{ATP} channel. Furthermore, PMA and carbachol abolished the increased gap junction permeability compared with nicorandil alone (Fig. 4). These findings suggest the involvement of PKCε in nicorandil-induced enhancement of gap junction communication.

Electrophysiological stimulation

To further elucidate the physiological effect of enhanced Cx43 level, ventricular pacing was performed. The arrhythmia score in
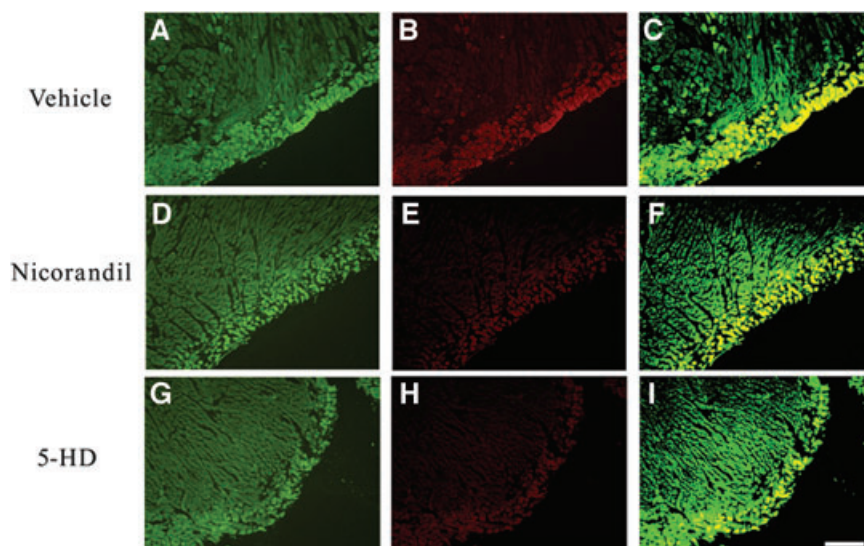

Fig. 6 Representative images of LV tissues from the border zone (≤ 2 mm within the infarct) stained with Lucifer yellow (green colour) and rhodamine-conjugated dextran (red colour). (**A**, **D** and **G**) Lucifer yellow staining and (**B**, **E** and **H**) rhodamine-conjugated dextran staining. (**C**, **F** and **I**) Merged images of Lucifer yellow and rhodamine-conjugated dextran staining. From (**A–C**) a vehicle-treated heart, (**D–F**) a nicorandil-treated heart and (**G–I**) a 5-HD–treated heart. Bars in the figures (magnification 100×) = 200 μm.
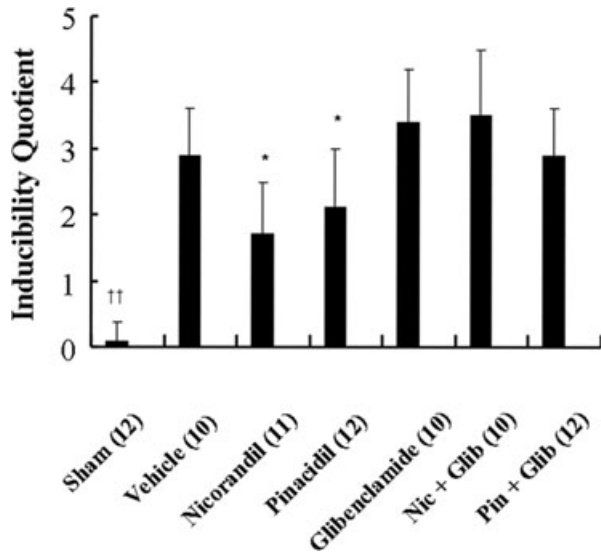
Fig. 7 Inducibility quotient of ventricular arrhythmias by programmed electrical stimulation four weeks after MI. The number of animals in each group is indicated in parentheses. $^*P < 0.05$ compared with vehicle-, glibenclamide (Glib)-, nicorandil (Nic) + Glib- and pinacidil (Pin) + Glib-treated groups. $^{\dagger\dagger}P < 0.01$ compared with infarcted groups.

the sham-operated rats was very low (0.08 ± 0.29; Fig. 7). Either nicorandil or pinacidil significantly decreased the inducibility of ventricular tachyarrhythmias compared with the vehicle. The beneficial effects of nicorandil and pinacidil on arrhythmic score were abolished by administering glibenclamide.

Discussion

This study shows for the first time that chronic treatment for 4 weeks with K_{ATP} channel agonists leads to preserved Cx43 distribution, phosphorylation, total amount and function, probably through PKCε-dependent phosphorylation of Cx43 on Ser368 in infarcted rats. The results were concordant for beneficial effects of K_{ATP} channel agonists, as documented structurally by an increase in immunofluorescence-stained Cx43, molecularly by myocardial Cx43 protein and mRNA levels, functionally by dye coupling and electrophysiologically by improvement of fatal ventricular tachyarrhythmias. We observed that the addition of the PKC activator, PMA and the specific PKCε agonist, carbachol, reversed Cx43 phosphorylation. Furthermore, addition of the PKC inhibitor chelerythrine, and the specific PKCε antagonist, εV1–2 did not have additional beneficial effects compared to nicorandil alone, suggesting a common pathway between nicorandil and PKC inhibitors.

The beneficial effect of K_{ATP} channel activation on arrhythmias was supported by three lines of evidence (Fig. 8).
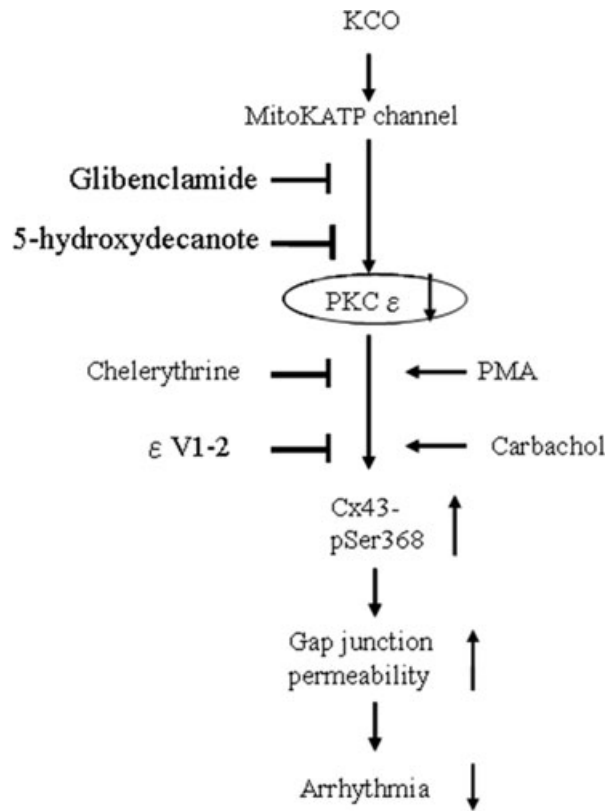

Fig. 8 Reaction sequences leading to attenuated arrhythmias. The diagram summarizes the immunofluorescent, molecular and pharmacological evidence presented in this report. εV1–2: myristoylated PKCε V1–2 peptide; KCO: potassium channel opener; PMA: phorbol 12-myristate 13-acetate. Inhibition of these signalling pathways by their respective inhibitors is indicated by the vertical lines.

1 Mitochondrial K_{ATP} channel activation played a role in modulating Cx43 after infarction. The alternation of Cx43 quantity, location and phosphorylation suggests that this protein is influenced by ventricular remodelling. Our results were consistent with the findings of Peters *et al.* [23], showing that in surviving border zone myocytes, there was an increased Cx43 deposition on lateral non-disk sarcolemmal membranes, leading to reentrant ventricular tachycardia [1,2]. Administration of K_{ATP} channel agonists attenuated reduced Cx43 level in chronically infarcted hearts. Because there were no significant differences in Cx43 level at the remote zone among the infarcted groups, attenuated reduced level of Cx43 at the border zone by administering K_{ATP} channel agonists reduced a morphological gradient of Cx43 level across the surviving post-infarction myocardium. Either pinacidil or nicorandil administration could attenuate reduced Cx43 level with a similar potency which may suggest that mitochondrial K_{ATP} channels play a role in regulating gap junctions. Although dissimilar structures, pinacidil and nicorandil appear to share a common mediator, Cx43, in which

transcription levels of Cx43 may play a role in the signal transduction pathway. The involvement of mitochondrial K_{ATP} channel activation in modulating Cx43 was further confirmed by administering a mitochondrial K_{ATP} antagonist (5-HD).

2 K_{ATP} channel agonists attenuated reduced Cx43 level through a PKCε-dependent pathway in chronically infarcted hearts. In this study, we demonstrated that PKCε activity was significantly increased after MI, consistent with the notion that post-infarction–induced stretch can activate PKC translocation from the cytosolic fraction to the membrane fraction. Both PMA and carbachol prevented the K_{ATP} channel agonist-induced increase in Cx43 phosphorylation and dye coupling, suggesting that PKCε is necessary for this event to occur. Because the general PKC inhibitor chelerythrine and PKCε-specific inhibitory peptide εV1–2 both exert a comparable effect on the activity of phospho-PKCε, PKCε might be the predominant PKC isoform that regulates the activity of Cx43. Furthermore, εV1–2 administration did not further increase Cx43 level compared with nicorandil alone, confirming the critical role of PKCε in nicorandil-mediated Cx43 level. In this study, the decreased activities of phospho-PKCε were associated with the increased level of Cx43-pSer368 and Cx43 phosphorylation. Our results were consistent with the findings of Liang *et al.* [24] and Sirnes *et al.* [25], which showed that PKC inhibition by 18-glycyrrhetinic acid increased Cx43-pSer368 in a dose-dependent manner and PKC activation by 12-*O*-tetradecanoylphorbol-13-acetate attenuated Cx43 level.

3 The severity of pacing-induced fatal arrhythmias was associated with Cx43 level. Our results showed that diminished Cx43 protein level may contribute to the initiation of fatal arrhythmias in the presence of a healed infarct. Downward remodelling of Cx43 showed high susceptibility to arrythmogenesis. Previous studies have shown that attenuated Cx43 level at the border zone was associated with an increase in wave break and alteration of reentrant wave front [26]. Increased Cx43 amount improves the conductivity, decreases the spatial heterogeneity of repolarization and reduces the vulnerability of infarcted hearts to fatal arrhythmias [27].

It appears from our study that the preserved Cx43 is related to an activation of K_{ATP} channels. The mechanisms by which K_{ATP} channel agonists attenuate ventricular remodelling remain to be defined. However, insulin levels cannot be a confounding factor. Although insulin secretion significantly increases in rats treated with glibenclamide as shown in this study and hyperinsulinemia has been shown to produce closure of gap junctions in a particle-receptor model [28], the increased insulin levels cannot be a confounding factor of Cx43 levels. When K_{ATP} channel agonists were administered, Cx43 levels were significantly increased with similar insulin levels compared with infarcted rats treated with vehicle, suggesting that factors other than insulin may contribute to the pathogenesis of enhanced Cx43 levels.

Phosphorylation of Cx43 is thought to be required for proper synthesis and assembly of connexins into gap junctions and to regulate electric conductance and permeability to small molecules [29]. Mutations at the phosphorylation site lead to the inability of the gap junction to respond to signalling cascades that would normally alter cell-to-cell communication [30]. In this study, K_{ATP} channel agonists inhibited remodelling-induced dephosphorylation of Ser368, which is considered important for the gating of Cx43 gap junction channels. There were contradictory observations regarding the effect of Cx43-pSer368 on cell coupling. Phosphorylation of Cx43 has been shown to be associated with both internalization of Cx43 and assembly of Cx43 into gap junctions [31]. Ek-Vitorin *et al.* [32] showed that phosphorylation of Cx43 at Ser368 markedly increases the permeability of the channel in normal rat kidney epithelial cells. In contrast, Cx43-pSer368 has been shown to reduce dye coupling in cultured fibroblasts [33]. Furthermore, Bupha-Intr *et al.* [34] showed that Cx43-pSer368 functions decrease the channel conductance of signals in normal physiological conditions with normal levels of Cx43; however, cell-to-cell communication is enhanced but subsequently lost when the levels of Cx43 are reduced. Thus, it is likely that the effect of Cx43 phosphorylation on the regulation of gap junction intercellular communication may be in a cell type–specific and temporal-dependent manner. We cannot exclude that K_{ATP} channel agonists could have also influenced intracellular trafficking of Cx43 or could have additionally affected the signalling pathways that modulate gap junctions. Regardless of its precise mechanism, this study provides the first evidence supporting the hypothesis that intercellular coupling and its modulation by K_{ATP} channel agonists can play a role in the mechanism of anti-arrhythmias.

Mechanisms

Previous studies have shown that high-energy phosphate levels and the expression of several proteins crucial to oxidative ATP production are significantly decreased at the border zone [35]. Thus, the capability of adapting cellular function and energy metabolism to varying physiological and pathological conditions in the context of low energy supply is vitally important. Cardiac K_{ATP} channels through tight integration with cellular metabolic signalling pathways respond with high fidelity to perturbations in cellular energetics [36]. In the heart, the K_{ATP} channel adjusts membrane potential-dependent cell functions to match the metabolic state [37]. Inhomogeneous alterations of expression and decreased activity of K_{ATP} channels in post-infarction failing myocardium occur during remodelling after MI [9]. K_{ATP} channels from remodelled hearts display an improper response to ATP, a reduced recognition of metabolic distress. Modulation of Cx43 channel function *via* phosphorylation is often linked with intracellular ATP levels [38]. Reduced ATP impedes phosphorylation, whereas due to ATP shortage, the dephosphorylation process is favoured [39]. Thus, K_{ATP} channel agonists have the potential to improve bioenergetic abnormalities and to prevent arrhythmias by re-establishing gap junctional intercellular communication.

Other mechanisms

Although this study suggests that the mechanisms of K_{ATP} channel agonists-induced attenuation of fatal arrhythmias may be related to attenuated reduced Cx43 level, other potential

mechanisms need to be studied. We have demonstrated that K_{ATP} channel agonists inhibit fatal arrhythmias by directly inhibiting sympathetic reinnervation [14], and by preventing cardiac fibrosis [40], thereby reducing the risk of isolated regional slowing of conduction and reentrant arrhythmias. Furthermore, K_{ATP} channels are important for the induction of abnormal automaticity and reentrant arrhythmias. The regional heterogeneity of K_{ATP} channel expression contributed to the regional heterogeneity in prolongation of the action potential in post-infarction remodelling [41]. K_{ATP} channel agonists improve regional differences in the action potential duration and attenuate arrhythmias. Preventing ionic remodelling may be an upstream approach to antiarrhythmic therapy.

Conclusions

These data show that a decrease in the level of PKCε by K_{ATP} channel agonist administration leads to up-regulation of Cx43-pSer368

linked with increased myocardial dye permeability and attenuated arrhythmia susceptibility after infarction. K_{ATP} channel agonists may represent a pharmacological principle with a clinical safety profile to prevent cardiac arrhythmias.

Acknowledgements

Conflict of interest

The authors confirm that there are no conflicts of interest.

References

1. **Weber KT, Anversa P**, **Armstrong PW, et al.** Remodeling and reparation of the cardiovascular system. *J Am Coll Cardiol.* 1992; 20: 3–16.

2. **Joyner RW.** Effects of the discrete pattern of electrical coupling on propagation through an electrical syncytium. *Circ Res.* 1982; 50: 192–200.

3. **Bennett MVL, Barrio LC, Bargiello TA, et al.** Gap junction: new tools, new answers, new questions. *Neuron.* 1991; 6: 305–20.

4. **Danik SB, Liu F**, **Zhang J**, **et al.** Modulation of cardiac gap junction expression and arrhythmic susceptibility. *Circ Res.* 2004; 95: 1035–41.

5. **Roell W, Lewalter T, Sasse P**, **et al.** Engraftment of connexin 43-expressing cells prevents post-infarct arrhythmia. *Nature.* 2007; 450: 817–24.

6. **Rottlaender D, Boengler K, Wolny M, et al.** Connexin 43 acts as a cytoprotective mediator of signal transduction by stimulating mitochondrial K_{ATP} channels in mouse cardiomyocytes. *J Clin Invest.* 2010; 120: 1441–53.

7. **Boengler K, Dodoni G, Rodriguez-Sinovas A, et al.** Connexin 43 in cardiomyocyte mitochondria and its increase by ischemic preconditioning. *Cardiovasc Res.* 2005; 67: 234–44.

8. **Naitoh K, Ichikawa Y, Miura T**, **et al.** MitoK_{ATP} channel activation suppresses gap junction permeability in the ischemic

myocardium by an ERK-dependent mechanism. *Cardiovasc Res.* 2006; 70: 374–83.

9. **Isidoro Tavares N, Philip-Couderc P, Papageorgiou I**, **et al.** Expression and function of ATP-dependent potassium channels in late post-infarction remodeling. *J Mol Cell Cardiol.* 2007; 42: 1016–25.

10. **Lampe PD, Lau AF.** Regulation of gap junctions by phosphorylation of connexins. *Arch Biochem Biophys.* 2000; 384: 205–15.

11. **Beardslee MA, Lerner DL, Tadros PN, et al.** Dephosphorylation and intracellular redistribution of ventricular connexin43 during electrical uncoupling induced by ischemia. *Circ Res.* 2000; 87: 656–62.

12. **Jabůrek M, Costa AD, Burton JR, et al.** Mitochondrial PKC epsilon and mitochondrial ATP-sensitive K^+ channel copurify and coreconstitute to form a functioning signaling module in proteoliposomes. *Circ Res.* 2006; 99: 878–83.

13. **Jiao J, Garg V, Yang B**, **et al.** Protein kinase C-epsilon induces caveolin-dependent internalization of vascular adenosine 5'-triphosphate-sensitive K^+ channels. *Hypertension.* 2008; 52: 499–506.

14. **Kang CS, Chen CC, Lin CC, et al.** Effect of ATP-sensitive potassium channel agonists on sympathetic hyperinnervation in postinfarcted rat hearts. *Am J Physiol Heart Circ Physiol.* 2009; 296: H1949–59.

15. **Xia QG, Chung O, Spitznagel H**, **et al.** Significance of timing of angiotensin AT1 receptor blockade in rats with myocardial

infarction-induced heart failure. *Cardiovasc Res.* 2001; 49: 110–7.

16. **Bélichard P, Savard P, Cardinal R, et al.** Markedly different effects on ventricular remodeling result in a decrease in inducibility of ventricular arrhythmias. *J Am Coll Cardiol.* 1994; 23: 505–13.

17. **Damron DS, Darvish A, Murphy L**, **et al.** Arachidonic acid-dependent phosphorylation of troponin I and myosin light chain 2 in cardiac myocytes. *Circ Res.* 1995; 76: 1011–9.

18. **Song JC, Rangachari PK, Matthews JB.** Opposing effects of PKC and PKC on basolateral membrane dynamics in intestinal epithelia. *Am J Physiol Cell Physiol.* 2002; 283: C1548–56.

19. **Pravdic D, Sedlic F, Mio Y**, **et al.** Anesthetic-induced preconditioning delays opening of mitochondrial permeability transition pore *via* protein Kinase C-ε-mediated pathway. *Anesthesiology.* 2009; 111: 267–74.

20. **Pfeffer MA, Braunwald E.** Ventricular remodeling after myocardial infarction. *Circulation.* 1990; 81: 1161–72.

21. **Herre JM, Wetstein L, Lin YL**, **et al.** Effect of transmural *versus* nontransmural myocardial infarction on inducibility of ventricular arrhythmias during sympathetic stimulation in dogs. *J Am Coll Cardiol.* 1988; 11: 414–21.

22. **Ruiz-Meana M, Garcia-Dorado D, Lane S**, **et al.** Persistence of gap junction

communication during myocardial ischemia. *Am J Physiol.* 2001; 280: H2563–571.

23. **Peters NS, Coromilas J, Severs NJ, *et al.*** Disturbed connexin43 gap junction distribution correlates with the location of reentrant circuits in the epicardial border zone of healing canine infarcts that cause ventricular tachycardia. *Circulation.* 1997; 95: 988–96.

24. **Liang JY, Wang SM, Chung TH, *et al.*** Effects of 18-glycyrrhetinic acid on serine 368 phosphorylation of connexin43 in rat neonatal cardiomyocytes. *Cell Biol Int.* 2008; 32: 1371–9.

25. **Sirnes S, Kjenseth A, Leithe E, *et al.*** Interplay between PKC and the MAP kinase pathway in Connexin43 phosphorylation and inhibition of gap junction intercellular communication. *Biochem Biophys Res Commun.* 2009; 382: 41–5.

26. **Ohara T, Ohara K, Cao JM, *et al.*** Increased wave break during ventricular fibrillation in the epicardial border zone of hearts with healed myocardial infarction. *Circulation.* 2001; 103: 1465–72.

27. **Amino M, Yoshioka K, Tanabe T, *et al.*** Heavy ion radiation up-regulates Cx43 and ameliorates arrhythmogenic substrates in hearts after myocardial infarction. *Cardiovasc Res.* 2006; 72: 412–21.

28. **Homma N, Alvarado JL, Coombs W, *et al.*** A particle-receptor model for the insulin-induced closure of connexin43 channels. *Circ Res.* 1998; 83: 27–32.

29. **Moreno AP**, **Saez JC**, **Fishman GI***, et al.* Human connexin43 gap junction channels: regulation of unitary conductances by phosphorylation. *Circ Res.* 1994; 74: 1050–7.

30. **Lampe PD, TenBroek EM, Burt JM, *et al.*** Phosphorylation of connexin43 on serine368 by protein kinase C regulates gap junctional communication. *J Cell Biol.* 2000; 149: 1503–12.

31. **Laird DW.** Connexin phosphorylation as a regulatory event linked to gap junction internalization and degradation. *Biochim Biophys Acta.* 2005; 1711: 172–82.

32. **Ek-Vitorin JF, King TJ, Heyman NS, *et al.*** Selectivity of connexin 43 channels is regulated through protein kinase C-dependent phosphorylation. *Circ Res.* 2006; 98: 1498–505.

33. **Bao X, Reuss L, Altenberg GA.** Regulation of purified and reconstituted connexin 43 hemichannels by protein kinase C-mediated phosphorylation of Serine 368. *J Biol Chem.* 2004; 279: 20058–66.

34. **Bupha-Intr T, Haizlip KM, Janssen PM.** Temporal changes in expression of connexin 43 after load-induced hypertrophy in vitro. *Am J Physiol Heart Circ Physiol.* 2009; 296: H806–14.

35. **Hu Q, Wang X, Lee J*, et al.*** Profound bioenergetic abnormalities in peri-infarct myocardial regions. *Am J Physiol Heart Circ Physiol.* 2006; 291: H648–57.

36. **Nichols CG.** K_{ATP} channels as molecular sensors of cellular metabolism. *Nature.* 2006; 440: 470–6.

37. **Tammaro P, Ashcroft FM.** Keeping the heart going: a new role for K_{ATP} channels. *J Physiol.* 2006; 577: 767.

38. **Turner MS, Haywood GA, Andreka P, *et al.*** Reversible connexin 43 dephosphorylation during hypoxia and reoxygenation is linked to cellular ATP levels. *Circ Res.* 2004; 95: 726–33.

39. **Verecchia F, Duthe F, Duval S, *et al.*** ATP counteracts the rundown of gap junctional channels of rat ventricular myocytes by promoting protein phosphorylation. *J Physiol.* 1999; 516: 447–59.

40. **Lee TM, Lin MS, Chang NC.** Effect of ATP-sensitive potassium channel agonists on ventricular remodeling in healed rat infarcts. *J Am Coll Cardiol.* 2008; 51: 1309–18.

41. **Isidoro Tavares N, Philip-Couderc P, Papageorgiou I**, *et al.* Expression and function of ATP-dependent potassium channels in late post-infarction remodeling. *J Mol Cell Cardiol.* 2007; 42: 1016–25.